Safety, Tolerability, and Efficacy Evaluation of the SlimME Device for Circumference Reduction

Giovanni Ferrando, MD*
Queen Anne Street Medical Centre, 18-22 Queen Anne St, Marylebone W1G 8HU, London

Objective: To assess the short- and long-term thermal impact of subclinical and clinical regimens of a single, non-invasive uniform ultrasound treatment session on subcutaneous adipose tissue (SAT).
Study Design: Prospective, open-label, single-arm, split-side study.
Methods: Patients ($n = 17$) were subjected to uniform ultrasound treatment, delivered in a single session with the SlimME device. The device was set to one of four treatment regimens, which differed in their durations and energy fluences during the raise and maintenance phases. Up to six abdominal regions were treated, with six patients receiving a different treatment on each side of the abdomen. Safety was assessed by measuring skin surface temperature, evaluating expected skin responses immediately and 30 min after treatment and via patient ratings of pain and discomfort. Efficacy of raising and then maintaining SAT temperatures at 48°C, was determined by routinely measuring SAT temperatures during the treatment session and by histological analysis of samples collected 7 ($n = 13$) or 90 ($n = 4$) days after treatment.
Results: Trace to mild erythema was observed in up to 48% of the treated zones, which, in most cases, resolved within 30 minutes. No significant rise in mean skin surface temperature ($\leq$26.5°C) was recorded following any of the four tested regimens. Overall, patients reported tolerability to treatment, with the highest mean pain score registered for the moderate and high intensity regimens (4.4 ± 1.5 and 4.9 ± 1.4, respectively). Mean SAT temperatures did not exceed 48.4 ± 2.5°C and were effectively maintained throughout the maintenance phase of the treatment session. Low-energy fluence led to localized fat coagulative necrotic lesions, surrounded by subacute rim of inflammation, while high-energy fluence induced fat coagulative necrosis alongside granulomatous panniculitis, which resolved within 90 days.
Conclusion: The tested uniform ultrasound regimens elicited SAT temperature elevations, with a subsequent energy-dependent increase in degree of fat necrosis. At the same time, the unique design spared the surrounding tissue from thermal damage and was associated with minimal discomfort. Taken together, the SlimME device constitutes an effective tool for destruction of stubborn hypodermal fat deposits. Lasers Surg. Med. 50:745–754, 2018. © 2018 The Authors. *Lasers in Surgery and Medicine* Published by Wiley Periodicals, Inc.

Key words: SlimME; non-invasive; ultrasound; fat reduction; fat cell destruction; subcutaneous fat; subcutaneous adipose tissue; lipolysis

INTRODUCTION

Due to the increasing prevalence of obesity, body contouring has become one of the most popular elective aesthetic procedures performed worldwide. Even with optimal dietary and workout regimens, some body areas, such as the abdomen, flanks, and thighs, present stubborn fat deposits that remain difficult to shape [1]. Metabolic disorders, such as congenital and acquired lipodystrophies, involving uneven distribution of fat, can also contribute to abnormal stubborn fat deposits that fail to respond to lifestyle changes. Invasive procedures, such as liposuction and abdominoplasty, can be deployed to permanently eliminate undesirable fat deposits. Yet, while these techniques have been upgraded to improve their safety profile, post-procedural complications, including infections, embolism, visceral perforations, seroma, nerve compression, changes in sensation, swelling, skin necrosis, burns, fluid imbalance, anesthesia-related toxicity, scars, and contour irregularities, are still common [2,3]. As a result, there is growing demand for non-invasive alternatives, with lower morbidity rates and shorter recovery times [4–10]. To date, the technologies most widely applied to non-invasively reduce localized subcutaneous adipose tissue (SAT) include cryolipolysis, radio-frequency (RF), and ultrasound [2]. Cryolipolysis elicits direct cold injury to adipocytes, resulting in lobular panniculitis and adipose tissue loss [11,12], whereas, RF and ultrasound

Conflict of Interest Disclosures: The author has completed and submitted the ICMJE Form for Disclosure of Potential Conflicts of Interest and none were reported.
Contract grant sponsor: Lumenis Ltd..

*Correspondence to: Giovanni Ferrando, MD, Queen Anne Street Medical Centre, 18-22 Queen Anne St, Marylebone W1G 8HU, London. E-mail: docferrando@gmail.com

Accepted 10 January 2018
Published online 7 February 2018 in Wiley Online Library (wileyonlinelibrary.com).
DOI 10.1002/lsm.22796

technologies induce thermal damage or non-thermal destruction of tissue by ultrasound waves [3,13–16].

Ultrasound is widely used in diagnostic and therapeutic applications [17–19]. Therapeutic ultrasound can induce a vast range of biological effects over a wide range of acoustic parameters. Ultrasound therapies can be grossly categorized [19,20] into low-power applications, which include sonophoresis, sonoporation, gene therapy and bone healing, and high-power applications, which include high-intensity focused ultrasound (HIFU) and lithotripsy. Unlike low-power ultrasound, which leads to temperature elevations of several degrees, inducing a temporary effect on the tissue, high-power ultrasound leads to elevated tissue temperatures to approximately 56–60°C, within seconds, causing instantaneous cell death.

Uniform ultrasound is a new non-invasive technology implemented in the SlimME device, which delivers uniform therapeutic ultrasound energy to the subcutaneous fat layer. The uniformity is achieved by aiming six collimated beams coming from different directions, toward the treated region. There, the energy is converted into heat by sound absorption, triggering thermal destruction of adipocyte cells. The temperatures reached by this procedure lie between those induced in classical low-power applications (42–50°C) and high-power applications (>56°C).

The system uses a continuous vacuum that pulls the tissue into the therapeutic head during treatment, holding it there to ensure targeted ultrasonic irradiation of the SAT lying beneath the skin surface, while sparing the surrounding organs (Fig. 1). During treatment, the therapeutic head is cooled to protect the epidermis and the upper dermal layers. This study aimed to define the thermal impact of various ultrasound energy intensities on the SAT, as assessed by histological analysis, skin temperature, skin responses, and patient-reported pain scores. Subjects underwent a single SlimME treatment session, 7 or 90 days before an abdominoplasty. SlimME-treated tissues were characterized by fat coagulative necrosis surrounded by granulomatous panniculitis and occasional apoptotic cell debris, 7 days following treatment, which could barely be observed 3 months following treatment.

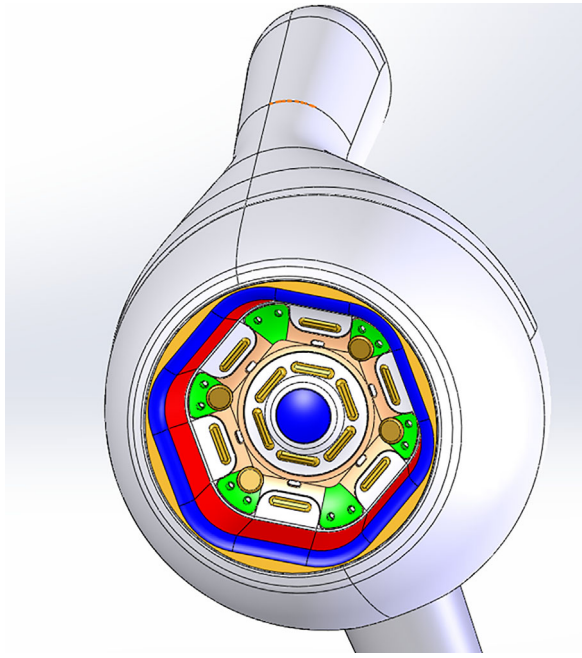

Fig. 1. Therapeutic hand piece design: Ultrasound transmission (red), vacuum (green), cooling system (blue).

MATERIALS AND METHODS

The study was conducted according to the principles of the Declaration of Helsinki and was approved by The Cosmetic Research Ethics Committee Ltd. (East Sussex, UK). All subjects provided written informed consent prior to participation.

This study was a 3-month, prospective, open-label, single-arm study in which all participants underwent a single abdominal treatment with the SlimME device.

Participants

Male and female patients, aged 18–65, with an abdominal fat thickness of at least 2.5 cm, scheduled to undergo abdominoplasty, were eligible to participate in the study. Heavy smokers (>1 pack of cigarettes per day) and patients with a history of surgery within 9 months of treatment, or planned surgery in the target area, participating in a clinical study of another investigational device within 3 months of enrollment or during the course of study, who had undergone previous ablative or non-ablative laser, radiofrequency or light therapy procedures in the areas to be treated, presenting local skin pathologies, or loss of natural structure in the treatment area or any general skin malfunction, bearing an implanted cardiac or any other implantable active device anywhere in the body, suffering from any significant systemic illness, and/or who consume more than 3 U a day of alcohol for men or 2 U per day for women, were excluded from the study. Pregnant women or women planning to become pregnant during the course of study, less than 3 months postpartum, lactating or less than 6 weeks after completion of breastfeeding, were also excluded.

Treatment Protocol

Seventeen (17) healthy subjects were allocated to one of two cohorts, according to their sequential enrollment into the study: (A) Thirteen (13) subjects received ultrasonic treatment 7 days (+3 days) prior to abdominoplasty, (B) four (4) subjects underwent treatment 90 days (±3 days) prior to abdominoplasty surgery. Subjects were subdivided to receive treatment regimens I and/or II or III and/or IV (detailed below), which differed in their durations and energy fluences during the raise and maintenance phases of treatment, as detailed below (patient allocation is detailed in Table 1). Subjects were treated in four to six 4 cm^2 abdominal zones, which is the effective dimension of

TABLE 1. Number of Treatment Zones Per Patient by Cohort

	Number of treatment zones per cohort						Number of temperature measurements in subcutaneous fat	
Patient ID	A-I	A-II	A-III	A-IV	B-III	B-IV	Regimen III	Regimen IV
1	2	2						
2	2	3						
3	2	2						
4		4						
5		4						
6		4						
7			4					
8			4					
9			4					
10			4					
11			2	2			2	2
12			3	3			3	3
13			2	4				
14						6		6
15						4		4
16					4		3	
17					4			
Total	6	19	23	9	8	10	8	15

the device handpiece. Each treatment area was assessed by imaging ultrasound to assure fat thickness of at least 2.5 cm. The contours of the treated area were marked with a surgical pen on a transparent sheet. Each zone was identified with a code. Lumenis coupling lotion was applied to each zone immediately prior to initiation of treatment, to allow for optimal transmission. After the therapeutic head was placed on the pre-marked skin surface, the device was activated at the appropriate pre-defined parameters.

Treatment Regimens

Regimen I: 177 J/cm^2 for the 72-second raise phase and 420-second maintenance phase (i.e., low intensity).

Regimen II: 207 J/cm^2 for the 72-second raise phase and the 540-second maintenance phase (i.e., mild intensity).

Regimen III: 237 J/cm^2 for the 72-second raise phase and the 660-second maintenance (i.e., moderate intensity).

Regimen IV: 146 J/cm^2 for the 96-second raise phase and 120-second maintenance phase (i.e., high intensity).

Cohort A: The effects of low and mild energy levels were compared by performing a split-abdomen treatment on three subjects, where Regimen I was delivered to the right side of the abdomen, and Regimen II to the left side of the abdomen. Another three subjects received treatment with the Regimen II setting on both sides of the abdomen. Four subjects received the Regimen III treatment on both sides of the abdomen, and three additional subjects received Regimen III treatment on the left side of the abdomen and Regimen IV treatment on the right side of the abdomen. All Cohort A patients underwent abdominoplasty 7 days following the SlimME treatment.

Cohort B: Two subjects received Regimen III treatment and two subjects receiving Regimen IV treatment. All Cohort B patients underwent abdominoplasty 90 days following the SlimME treatment.

Device Description

SlimME is a non-invasive transcutaneous ultrasound system prototype (LUMENIS, Ltd., Yoqneam, Israel), indicated for thermal induction of adipocyte death.

The ultrasound-therapeutic head is a manual, handheld unit, with an interior hexagonal shaped chamber (Fig. 1), enabling an effective treatment volume of $\sim$7 cm^3 within the SAT. It is designed to draw up the tissue, using a vacuum mechanism (18 in Hg), into the head's chamber cavity, to assure both (i) effective coupling between the skin surface and the therapeutic transducers and (ii) transmission of the ultrasonic energy parallel to the skin surface, which minimizes the possibility of heating undesired targets. The perpendicular walls of the interior side of the handpiece consist of three parallel pairs of 2 MHz ceramic transducers, arranged in the hexagonal shape (Fig. 1). Skin contact sensors located along the handpiece's walls assure full contact between the skin/acoustic coupler and the ultrasonic elements. The ceramics are synchronized to transmit acoustic energy one at a time, to maximize the effect in the targeted area, while avoiding overheating of the surrounding skin layers. A water cooling system, located at the top of the transducer cavity, is set to a range of 18–21°C and thus prevents temperature elevations above body temperature in the skin layers during the treatment.

The ultrasonic treatment is divided into two phases: the "raise phase," during which the temperature in the SAT is elevated to a desired target temperature (48°C), followed by the "maintenance phase," when the target temperature achieved at the end of the raise phase is maintained constant over time, to induce a thermal effect on the tissue. In each of the two phases, acoustic energies and time durations can be adjusted to suit specific treatment goals.

Safety Assessments

Skin surface temperature was measured during the treatment, using an infra-red thermometer aimed at the skin surface of randomly selected treatment zones: 6 treatment zones of Regimen I, 19 treatment zones of Regimen II, 5 treatment zones of Regimen III, and 11 treatment zones of Regimen IV.

Expected skin responses (i.e., erythema, edema, purpura, and hematoma) were graded by the investigator on a five-point scale (0 = none; 1 = trace; 2 = mild; 3 = moderate; 4 = severe), immediately and 30 minutes following treatment.

Procedure-associated pain and discomfort were scored by subjects immediately following treatment procedures, using a ten-point visual analogue scale (VAS), where "0" indicated "no pain" and 10 "intolerable pain."

SAT Temperature Assessment

Once the therapeutic ultrasound handpiece was placed on each treatment zone and vacuum was applied, a 26 ga (0.018″) sterile thermocouple, equipped with a 4 cm needle (MT-26/4, maximum temperature: 200°C; Physitemp, Clifton, NJ) was inserted through the top central area of the therapeutic head, into the fat layer, to a depth of 15 mm beneath the skin surface, following skin surface sterilization. Temperature measurements in the ultrasound-treated zones within SAT were recorded in a temperature logger, every two seconds throughout the raise and maintenance phases. The thermocouple needle was withdrawn at the end of treatment session, prior to vacuum release.

Histological Assessment

Skin and underlying fat tissue samples were collected for histopathological assessment 7 (group A; $n = 13$) or 90 (group B; $n = 4$) days following treatment, during the abdominoplasty procedure, immediately following abdomen excision. The excised tissue samples were immersed in Baker fixative solution at room temperature. Tissue samples were then embedded in paraffin blocks, cut to 5 ± 0.5 μm-thick sections, using a microtome (Microm Microtech, Brignais, France), and stained with hematoxylin eosin (H&E). The histopathologic evaluation was conducted by NAMSA (Lyon, France), in accordance with the ISO10993-6 standards. Sections ($n = 722$) were viewed under a NIKON microscope Eclipse E80i, equipped with ×2, ×4, ×10, ×20, ×40, and ×60 objectives. The following parameters were qualitatively evaluated: inflammatory reaction (macrophages, lymphocytes, plasma cells, polymorphonuclear cells, and giant cells), fat coagulative necrosis, apoptotic bodies, septal fibrosis, muscle degeneration, hemorrhage, congestion and/or edema, vascular necrosis and/or inflammation, epidermal degenerative/necrotic changes, and dermal degenerative changes.

Safety Assessments

Adverse event monitoring was conducted throughout the study and included hematological evaluations (white blood cells, red blood cells, hemoglobin, hematocrit, mean corpuscular volume (MCV), mean cell hemoglobin (MCH), mean corpuscular hemoglobin concentration (MCHC), platelets, differential count) on days 1, 7, 30, 60, and 90 following ultrasonic treatments, biochemistry evaluations (creatinine, calcium, glucose, cholesterol, total protein, globulin, aspartate aminotransferase (AST), lactate dehydrogenase (LDH), potassium, creatine kinase (CPK), phosphorus, urea, amylase, albumin, total bilirubin, alanine transaminase (ALT), gamma-glutamyl transpeptidase (GGT), sodium, chloride, triglycerides, lactate dehydrogenase (LDH), and free fatty acids), evaluated on days 1, 2, 3, 7, 30, 60, and 90 following the procedure, and coagulation function on days 7 and 90 following treatment. All abdominoplasty operations were performed by the same surgeon, and all measures were compared to baseline levels (pretreatment).

Statistical Methods

This study was planned as a feasibility study and was not statistically powered to test a hypothesis. The sample size of 17 subjects, having a total number of 75 treatment zones, in one of four possible treatment regimens was considered sufficient to obtain estimates of the desired safety variables. All statistical analyses of safety and efficacy measures are summarized in tables or figures via descriptive statistics. Continuous variables are summarized by a mean and standard deviation, and categorical variables by a count and percent and 95% Wilson Score confidence interval. VAS and temperature measurements were modeled with a repeated measures analysis of variance model; this was done in order to take into consideration the multiple areas treated per subject, model estimated means (LSmeans) with respective standard deviations (calculated from the variance components of the models) as well as level of significance comparing LSmean differences.

RESULTS

All 17 screened subjects (16 females and 1 male) met the initial inclusion criteria, were enrolled in the study and completed all follow-up evaluations, including the safety evaluation. All subjects were Caucasian, with a mean age of 46.9 ± 10.9 and mean BMI of $28.8 \pm 4.8\,kg/m^2$ (Table 2). On average, each subject was treated in 4–6 abdominal zones.

Trace to mild erythema was observed immediately following treatment (Table 3), with erythema occurring in only 32% of Regimen I-treated zones, and in 48% and

TABLE 2. Demographic and Baseline Clinical Characteristics

Demographic and clinical characteristics	$n = 17$
Age, yr (mean [SD])	46.9 (10.9)
BMI, kg/m^2 (mean [SD])	28.8 (4.8)
Female, n (%)	16 (94)
Caucasian %	100

BMI, body mass index.

45% of the Regimen II-treated and Regimen III-treated regions, respectively. Regimen IV in Cohorts A and B was associated with the lowest incidence of erythema (24%). All cases of erythema following Regimen I, II and IV fully resolved within 30 minutes of treatment, and only 9% of Regimen III-treated zones in both Cohorts A and B still showed signs of erythema at the 30 minutes follow-up (Table 3). Edema, purpura, and hematoma were not observed in any of the treated zones.

Skin surface temperature measurements, recorded during ultrasound transmission, were highly similar across treatment regimens (25 ± 0.8, 24.3 ± 0.8, 25.6 ± 0.6, and 24.9 ± 0.5°C for Regimens I, II, III, and IV, respectively; Table 4). The highest skin surface temperature following treatment (26.5°C) was recorded following treatment with Regimen III.

The average VAS score was 3.1 ± 0.8 ($n = 6$), 2.5 ± 2.3 ($n = 19$), 4.4 ± 1.5 ($n = 31$), and 4.9 ± 1.4 ($n = 17$) for Regimens I, II, III, and IV, respectively (Fig. 2), with no significant differences noted between regimens (F-$(3,3) = 1.55$; $P = 0.3647$). No interpatient consistency was noted for pain scores at specific treatment zones; no zone could be associated with a higher pain score as compared to another zone.

No major adverse events were noted by the study physician, and the subjects maintained good health throughout the study. A single treatment-unrelated and device-unrelated report of dizziness, accompanied by a drop in blood cells count, was recorded on the day of abdominoplasty, performed 90 days following the SlimME treatment; the surgeon classified it as a panic attack due to the upcoming surgery.

Blood evaluations confirmed that the treatment had minimal and insignificant effects on subjects; no clinically significant changes from baseline were noted in any of the tested parameters on days 1 and 7 in Cohort A and on days 7, 30, 60, and 90 following treatments in Cohort B. A gradual rise in CK levels from 262 IU/L at baseline to 978 IU/L on day 7 (data not shown) was noted in one Cohort A patient (Regimens I and II), however, she reported increased muscle activity during this period. Similarly, treatment had minimal, and clinically insignificant effects on blood lipid levels.

Temperature measurements within the SAT, measured in 23 zones (Table 1) demonstrated an elevation to 44.9 ± 2.7°C ($n = 8$) by the end of the Regimen III raise phase (72 seconds) and to 48.4 ± 2.5°C ($n = 15$) by the end of

TABLE 3. Immediate and Late Skin Response in Each Zone to Treatment; n, (%) and [95% Wilson Score Confidence Interval]

	Regimen	I ($n = 6$)		II ($n = 19$)		III ($n = 31$)		IV ($n = 17$)	
	Severity	Trace	Mild	Trace	Mild	Trace	Mild	Trace	Mild
Erythema	Immediate response	1 (16%) [3.01%;56.35%]	1 (16%) [3.01%;56.35%]	7 (37%) [19.15%;58.96%]	2 (11%) [2.94%;31.39%]	11 (35%) [21.12%;53.05%]	3 (10%) [3.35%;24.90%]	4 (24%) [9.56%;47.26%]	0 (0%) [0.00%;18.43%]
	30 minutes	0 (0%) [0.00%;39.03%]	0 (0%) [0.00%;39.03%]	0 (0%) [0.00%;16.82%]	0 (0%) [0.00%;16.82%]	2 (6%) [1.79%;20.72%]	1 (3%) [0.57%;16.19%]	0 (%) [0.00%;18.43%]	0 (%) [0.00%;18.43%]
Edema	Immediate response	0 (0%) [0.00%;39.03%]	0 (0%) [0.00%;39.03%]	0 (0%) [0.00%;16.82%]	0 (0%) [0.00%;16.82%]	0 (0%) [0.00%;11.03%]	0 (0%) [0.00%;11.03%]	0 (%) [0.00%;18.43%]	0 (%) [0.00%;18.43%]
Purpura	Immediate response	0 (0%) [0.00%;39.03%]	0 (0%) [0.00%;39.03%]	0 (0%) [0.00%;16.82%]	0 (0%) [0.00%;16.82%]	0 (0%) [0.00%;11.03%]	0 (0%) [0.00%;11.03%]	0 (%) [0.00%;18.43%]	0 (%) [0.00%;18.43%]
Hematoma	Immediate response	0 [0.00%;39.03%]	0 [0.00%;39.03%]	0 (0%) [0.00%;16.82%]	0 (0%) [0.00%;16.82%]	0 (0%) [0.00%;11.03%]	0 (0%) [0.00%;11.03%]	0 (%) [0.00%;18.43%]	0 (%) [0.00%;18.43%]

TABLE 4. Skin Surface Measured Temperature Immediately Following Treatment

Disribution of skin surface temperature immediately after treatemnt	*n*	Mean	SD	Minimum	Median	Maximum
Subject #						
1	4.0	25.0	1.1	23.5	25.2	25.9
2	5.0	24.6	1.4	22.7	24.5	26.0
3	4.0	24.0	0.9	23.4	23.7	25.3
4	4.0	24.4	0.3	24.1	24.3	24.9
5	4.0	24.4	0.6	23.7	24.4	25.1
6	4.0	24.4	0.5	24.0	24.3	25.2
7	4.0	25.8	0.5	25.3	25.8	26.5
8	4.0	25.2	0.8	24.4	25.1	26.1
9	4.0	25.3	0.2	25.1	25.3	25.6
10	4.0	26.0	0.1	25.8	26.0	26.1

the Regimen IV raise phase (96 seconds) (Fig. 3A and B). The average temperatures recorded throughout the maintenance phases of both regimens remained relatively constant over time, with a mean $43.9 \pm 3.7^{\circ}$C recorded at the end of Regimen III treatment and $47.8 \pm 3.3^{\circ}$C following Regimen IV (Fig. 3A and B). No statistically significant difference in raise phase or maintenance phase temperatures was observed between the regimens ($P > 0.06$).

A total of 75 treatment zones were histologically analyzed (Table 1). Histopathologic assessment of the treated zones revealed well demarcated, linear lesions 5–25 mm under and parallel to the skin surface (data not shown). SAT subjected to low energy fluence (Regimen I) displayed focal regions of fat coagulative necrosis, characterized by the absence of nuclei (Fig. 4) and by the presence of occasional apoptotic cell debris (data not shown). The necrotic areas were surrounded by a thin rim of subacute inflammation, characterized by congested capillaries and several inflammatory cells (lymphocytes, macrophages, and polymorphonuclear cells). Both fat coagulative necrosis and peripheral inflammation correlated with the ultrasonic treatment boundaries. No unusual histopathologic findings were noted in Regimen II samples (mid-energy fluence; $n = 19$). Two samples showed minimal granulomatous panniculitis (data not shown), but any relationship to treatment was considered doubtful in view of the lack of a well-defined linear shape in this lesion, as well as the negligible severity.

Histopathologic findings, including focal areas of fat coagulative necrosis surrounded by granulomatous panniculitis and occasional apoptotic cell debris (Fig. 4), were noted in almost all evaluated Regimen III- and Regimen IV-treated zones ($n = 32$). In addition, multifocal granulomatous inflammation, characterized by seemingly empty vacuoles (500–800 μm in diameter), surrounded by a single layer of macrophages and multinucleated giant cells, was frequently observed. Slight to moderate vascular necrosis was observed in the coagulative necrotic areas of all Regimen III- and Regimen IV-treated zones (data not shown). No significant histopathological differences were noted between zones treated with Regimen III ($n = 23$) versus Regimen IV ($n = 9$) settings (Fig. 4).

In most of the zones evaluated 90 days following treatment, histopathologic abnormalities were only observed in the SAT of one out of four subjects. In this subject, residual panniculitis accompanied by septal fibrotic tissue and vacuoles, was observed in two out of six treated zones (Fig. 5).

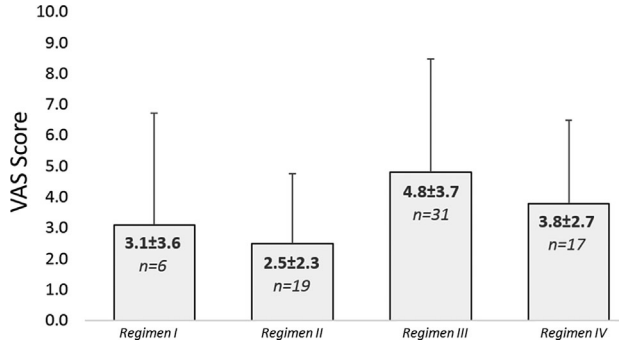

Fig. 2. Patient-rated treatment-associated pain and discomfort. Mean patient-rated pain and discomfort (±standard deviation) in each treatment zone, using a visual analogue scale (VAS), ranging from "0" to "10" ("no pain" to "intolerable pain," respectively).

DISCUSSION

The current study was the first clinical study aiming to evaluate the histological effect of controlled, multi-element, non-focused, clinical, and sub-clinical ultrasound treatment on the subcutaneous fat layer over a period of up to 90 days following treatment. The Uniform Ultrasound technology was designed to induce temperature variations, which, in turn, trigger metabolic and structural modifications in the SAT. These alterations directly impact the mechanical properties of the treated tissue and lead to short-term and long-term volumetric alterations [21–25].

Franco et al. showed that adipocyte viability in culture dropped significantly from 89% to 20% following a 1 minute-long temperature increase from 45 to 50°C, whereas, a 3-minute exposure to 45°C resulted in 40%

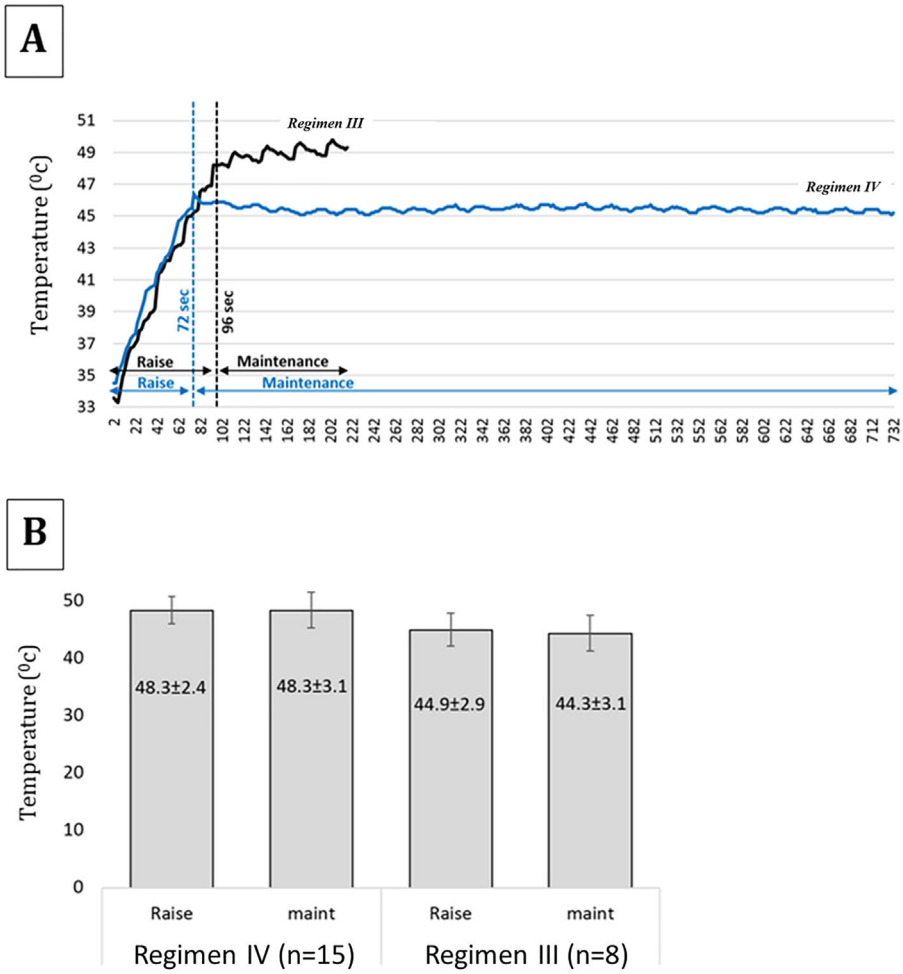

Fig. 3. Temperature measurements within SAT (**A**) representative recording of SAT temperatures during the two phases of treatments. The raise and maintenance phases of Regimen III are shown in blue (72 and 660 seconds, respectively) and of Regimen IV in black (96 and 120 seconds, respectively). (**B**) Mean SAT temperatures (±standard deviation) at the end of raise and maintenance (maint) phases of Regimens III and IV, in Cohorts A and B.

viability of cells [25]. In addition, temperature measurements performed on SAT taken from abdominoplasty patients, demonstrated that increasing the SAT temperature to approximately 45°C for 15 minutes resulted in vascular alterations, first detectable 4 days after treatment, followed by fat necrosis and infiltration of foamy macrophages within 9 days [25]. The SlimME system was designed to elevate the SAT temperature to a range between 45 and 48°C and to maintain these temperatures over a clinically meaningful period, exceeding adipocyte tolerability and ultimately leading to cell death. SAT temperature measurements at the end of the SlimME raise phases of Regimens III and IV were 44.9 and 48.4°C, respectively, confirming the accuracy of the projected temperature. In addition, the system settings enabled maintenance of these target temperatures over periods of 660 and 120 seconds, for Regimens III and IV, respectively. The mean temperature measurements at the end of these maintenance phases were 43.9 and 47.8°C, respectively.

SlimME-treated tissues were characterized by fat coagulative necrosis surrounded by granulomatous panniculitis and occasional apoptotic cell debris, 7 days following treatment (Cohort A), which could barely be observed 3 months following treatment (Cohort B). The histological evaluation showed an energy dose-dependent thermal effect, as demonstrated by the ultrasonic effect seen in all Cohort A-III zones, which was absent in the vast majority of zones treated with sub-therapeutic energy doses (Cohorts A-I and A-II).

The most prevalent complications of high intensity ultrasound are rooted in the elevation in tissue temperatures to >56°C, which is associated with pain, high incidence of adverse effects and discomfort, which can be prolonged [26]. It is generally assumed that lower energy settings can reduce these unwanted consequences without

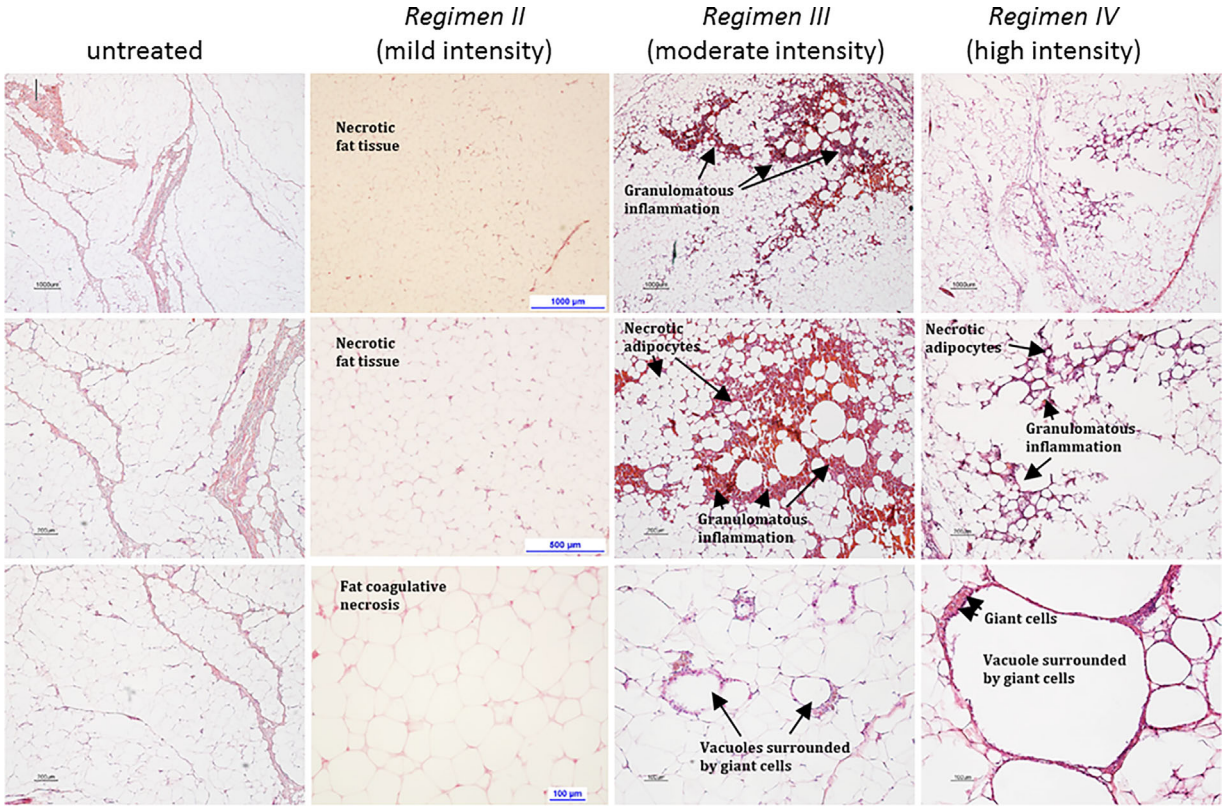

Fig. 4. Histological analysis 7 days following ultrasonic treatments (Cohort A). Tissue samples were collected 7 days following treatment, processed and stained with H&E.

hampering efficacy, as demonstrated in the present study. Six synchronized irradiating ceramics of the device, sequentially transmit the acoustic energy under vacuum, which enables treatment of the SAT parallel to the skin surface. At the same time, the cooling system avoids heat accumulation in the skin layers, enhancing treatment safety. The advantages of these protective features were reflected in skin temperature, which did not exceed 26.5°C, and remained far below the tissue damage threshold in all evaluated settings. The temperature measurements on the skin surface correlated well with the absence of skin response following treatments; no burns, blisters, purpura, or hematoma were observed in any of the treated zones. Only trace to mild erythema was seen immediately following treatment in 32%, 48%, and 45% of zones treated with low, mild and moderate energy doses, respectively; almost all cases were fully resolved within 30 minutes.

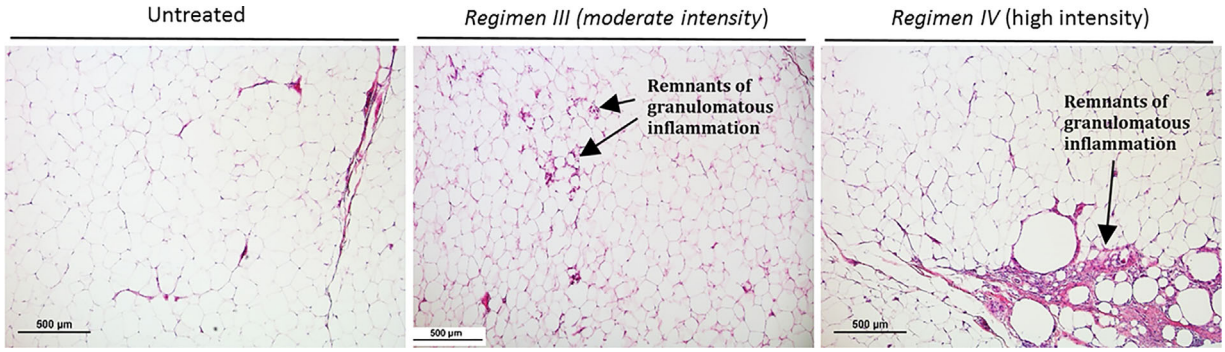

Fig. 5. Histological analysis 90 days following ultrasonic treatment (Cohort B). Tissue samples were collected, processed, and stained with H&E 90 days following ultrasound treatment with Regimens III (moderate intensity) or IV (high intensity).

The clinical effect of the SlimME treatment has been recently tested on 21 subjects, in an open-label, single-arm exploratory study [27]. Circumference measurements in the anterior superior iliac spine (ASIS), in the umbilicus and under the ribs, showed a reduction of 3.2 ± 0.7, 3.9 ± 0.7, and 3.3 ± 0.8 cm, respectively, at 3 months following a single treatment in the abdomen. Blinded evaluation of circumference showed that 87.5% of the "pre-treatment" versus "post-treatment" photographs were correctly categorized by two independent reviewers, with 92% of subjects classifying their conditions as either improved or much improved within this same time period. Treatment safety was similar to that recorded in the current study, with all immediate skin reactions falling within the expected norms, all being short-lived and self-resolving.

As this study was designed to assess feasibility, interpretation of the outcomes is limited by the small number of subjects, which does not provide statistical power to detect significant differences between treatment regimens. Further larger scale studies will be required to explore such differences.

CONCLUSION

This study is one of the few studies published so far, evaluating the impact and safety of non-invasive ultrasound-based modality for fat tissue destruction. The work demonstrated the local and systemic safety of the SlimME treatment, resulting in the destruction of the targeted fat cells, with minimal discomfort to patients. More specifically, controllable fine-tuning of the target end-point temperature in the adipose soft tissue, the acoustic power and the duration of temperature maintenance dictated the extent of lesions created in the SAT. The clinical ultrasound settings evaluated in this study (Regimens III and IV) resulted in demarcated lesions within the SAT, whereas, the sub-clinical settings (Regimens I and II) did not induce such an effect in the tissue. In addition, unlike high ultrasonic energy levels applied from a single element, which rapidly induce above-threshold tissue temperatures, resulting in immediate cell death, the SlimME system delivers the acoustic energy intermittently, from six independent elements under vacuum, with topical cooling. Together, a gradual increase of temperature is achieved in the target area and underlying region, sparing the surrounding tissue and skin from thermal damage and from thermally induced nociception. The advantages demonstrated in this study may be of clinical relevance in the pursuit for a high-end ultimate solution for destruction of stubborn hypodermal fat deposits in healthy subjects seeking circumference reduction.

ACKNOWLEDGMENTS

The author is grateful to Dr. Yehudit Posen for her valuable and constructive suggestions during the data consolidation and paper writing, to Dr Lisa Deutsch, for her important statistical analysis of the data, as well as to Dr. Natalie Dror, from Lumenis, for her great technical assistance with the submission procedure.

REFERENCES

1. Leal H, Cantu P. In: Katz B, Sadick N, editors. Procedures in Cosmetic Dermatology Series: Body Contouring. Elsevier; 2010. pp 107–121.
2. Kennedy J, Verne S, Griffith R, Falto-Aizpurua L, Nouri K. Non-invasive subcutaneous fat reduction: a review. J Eur Acad Dermatol Venereol 2015;29(9):1679–1688.
3. Brown SA, Greenbaum L, Shtukmaster S, Zadok Y, Ben-Ezra S, Kushkuley L. Characterization of nonthermal focused ultrasound for noninvasive selective fat cell disruption (lysis): Technical and preclinical assessment. Plast Reconstr Surg. 2009;124(1):92–101.
4. Kelley DE. Thermodynamics, liposuction, and metabolism. N Engl J Med 2004;350(25):2542–2544.
5. Kenkel JM, Lipschitz AH, Shepherd G, et al. Pharmacokinetics and safety of lidocaine and monoethylglycinexylidide in liposuction: a microdialysis study. Plast Reconstr Surg 2004;114(2):516–525.
6. Lipschitz AH, Kenkel JM, Luby M, Sorokin E, Rohrich RJ, Brown SA. Electrolyte and plasma enzyme analyses during large-volume liposuction. Plast Reconstr Surg 2004;114(3): 766–775.
7. Rohrich RJ, Leedy JE, Swamy R, Brown SA, Coleman J. Fluid resuscitation in liposuction: a retrospective review of 89 consecutive subjects. Plast Reconstr Surg 2006;117(2): 431–435.
8. Trott SA, Beran SJ, Rohrich RJ, Kenkel JM, Adams WP, Jr., Klein KW. Safety considerations and fluid resuscitation in liposuction: an analysis of 53 consecutive subjects. Plast Reconstr Surg 1998;102(6):2220–2229.
9. ASPRS Task Force on Lipoplasty, J. G. Bruner (Chair). 1997 Survey Summary Report. Arlington Heights, Ill.: American Society of Plastic and Reconstructive Surgeons, 1998.
10. Co AC, Abad-Casintahan MF, Espinoza-Thaebtharm A. Submentalfat reduction by mesotherapy using phosphatidylcholinealone vs phosphatidylcholine and organic silicium: a pilot study. J Cosmet Dermatol 2007;6:250–257.
11. Kennedy JE, Ter Haar GR, Cranston D. High intensity focused ultrasound: surgery of the future? Br J Radiol 2003; 76(909):590–599.
12. Stebbins WG, Hanke CW, Petersen J. Novel method of minimally invasive removal of large lipoma after laser lipolysis with 980nm diode laser. Dermatol Ther 2011;24(1):125–130.
13. Weiss R, Weiss M, Beasley K, Vrba J, Bernardy J. Operator independent focused high frequency ISM band for fat reduction: porcine model. Lasers Surg Med 2013;45:235–239.
14. Jewell ML, Solish NJ, Desilets CS. Noninvasive body sculpting technologies with an emphasis on high-intensity focused ultrasound. Aesthetic Plast Surg 2011;35:901–912.
15. Paul M, Blugerman G, Kreindel M, Mulholland RS. Three-dimensional radiofrequency tissue tightening: a proposed mechanism and applications for body contouring. Aesthetic Plast Surg 2011;35:87–95.
16. Friedmann DP, Bourgeois GP, Chan HHL, Butterwisk KJ. Complications from microfocused transcutaneous ultrasound: case series and review of the literature. Lasers Surg Med 2018;50(1):13–19.
17. Guillory RK, Gunter OL. Ultrasound in the surgical intensive care unit. Curr Opin Crit Care 2008;14:415–422.
18. Lockhart ME, Robbin ML. Renal vascular imaging: ultrasound and other modalities. Ultrasound Q 2007;23:279–292.
19. Ferraro GA, De Francesco F, Nicoletti G, Rossano F, D'Andrea F. Histologic effects of external ultrasound-assisted lipectomy on adipose tissue. Aesthetic Plast Surg 2008;32:111–115.
20. Illouz YG. Illouz's technique of body contouring by lipolysis. Clin Plast Surg 1984;11(3):409–417.
21. Gage AA, Caruana JA, Jr, Montes M. Critical temperature for skin necrosis in experimental cryosurgery. Cryobiology 1982;19(3):273–282.
22. Manstein D, Laubach H, Watanabe K, Farinelli W, Zurakowski D, Anderson RR. Selective cryolysis: a novel method of non-invasive fat removal. Lasers Surg Med 2008;40(9): 595–604.
23. Zelickson B, Egbert BM, Preciado J, Allison J, Springer K, Rhoades RW, Manstein D. Cryolipolysis for noninvasive fat

cell destruction: initial results from a pig model. Dermatol Surg 2009;35(10):1462–1470.
24. Meshorer A, Prionas SD, Fajardo LF, Meyer JL, Hahn GM, Martinez AA. The effects of hyperthermia on normal mesenchymal tissues. Application of a histologic grading system. Arch Pathol Lab Med 1983;107(6):328–334.
25. Franco W, Kothare A, Ronan SJ, Grekin RC, McCalmont TH. Hyperthermic injury to adipocyte cells by selective heating of subcutaneous fat with a novel radiofrequency device: feasibility studies. Lasers Surg Med 2010;42(5): 361–370.
26. Wu F, Wang ZB, Chen WZ, et al. Extracorporeal high intensity focused ultrasound ablation in the treatment of 1038 patients with solid carcinomas in China: an overview. Ultrason Sonochem 2004;11(3–4):149–154.
27. Otto MJ. The safety and efficacy of thermal lipolysis of adipose tissue via ultrasound for circumference reduction: an open label, single-arm exploratory study. Lasers Surg Med 2016;48(8):734–741.